Bioorganic Chemistry 88 (2019) 102948

Contents lists available at ScienceDirect

Bioorganic Chemistry

journal homepage: www.elsevier.com/locate/bioorg

Magmenthanes A-H: Eight new meroterpenoids from the bark of *Magnolia officinalis* var. *Biloba*

Chuan Li, Chuang-Jun Li, Jie Ma, Ji-Wu Huang, Xu-Yan Wang, Xiao-Liang Wang, Fei Ye, Dong-Ming Zhang*

State Key Laboratory of Bioactive Substance and Function of Natural Medicines, Institute of Materia Medica, Chinese Academy of Medical Sciences and Peking Union Medical College, Beijing 100050, People's Republic of China

ARTICLE INFO

Keywords:
Magnolia officinalis var. *biloba*
Meroterpenoid
PTP1B inhibitory

ABSTRACT

Eight new meroterpenoids with different types of monoterpene units, namely, magmenthanes A-H (**1**–**8**), were identified from the bark of *Magnolia officinalis* var. *biloba*. Magmenthane A (**1**) possesses a 1,3-dioxabicyclo [4.3.0^{1,5}] nonane skeleton, **1**–**5** possess five pairs of enantiomers and **6** possesses a 1,1′-diallyl-biphenyl fragment. The structures of **1**–**8** were elucidated on the basis of 1D and 2D NMR, HRESIMS and electronic circular dichroism (ECD) calculations. Compounds **5** and **8** displayed significant PTP1B inhibitory activities with IC_{50} values of 4.38 and 3.88 μM, respectively.

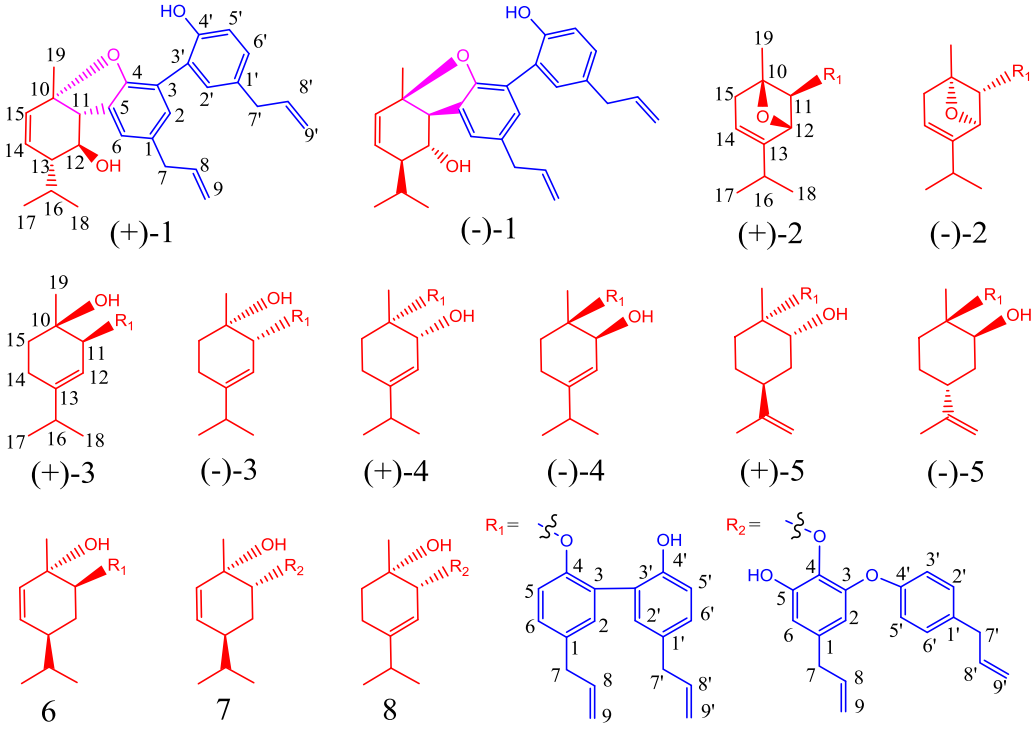

* Corresponding author.
E-mail address: zhangdm@imm.ac.cn (D.-M. Zhang).

https://doi.org/10.1016/j.bioorg.2019.102948
Received 3 January 2019; Received in revised form 14 February 2019; Accepted 21 April 2019
Available online 27 April 2019

1. Introduction

The bark of *Magnolia officinalis* [1] (*Magnolia officinalis* Rehd. et Wils or *Magnolia officinalis* Rehd. et Wils var. *biloba*) has been used as an important traditional Chinese medicine for the treatment and prevent diseases, such as abdominal distension and phlegm, for centuries in China. The main secondary metabolites of *Magnolia officinalis* include neolignanes [2–4], phenylethanoid glycosides [5,8], alkaloids [6–8] and terpenoids [9]. Pharmacological investigations on the chemical constitution of *M. officinalis* include explorations of its anti-inflammatory [10], antidepressant [11,12], and neurotropic [9] properties, along with its UVB-induced phototoxicity [13]. This is only a part of our continuous endeavour to search for more biological metabolites from traditional Chinese medicine. The *Magnolia officinalis Rehd.* et Wills var. *biloba* (*Magnolia officinalis* var. *biloba*.) plant, one of two species of *Magnolia officinalis* [14,15], has attracted more attention from our group. Previous phytochemical investigation on the bark of *M. officinalis* var. *biloba* was reported regarding three polycyclic meroterpenoids [9]. In our continuous work, five new pairs of enantiomers **1**–**5** and compounds **6**–**8** were isolated from the 95% ethanolic extract of the bark of *Magnolia officinalis* var. *biloba*. Compounds **1**–**8** possess different types of *p*-methane moieties [16]. Furthermore, enantiomers **1**–**5** were further separated through HPLC using an AD-H column. We believe that the enantiomers of compounds **6**–**8** were not encountered in this study, while compounds **1**–**5** were isolated as racemic mixtures from the plant. Hence, the detailed information of isolation, structure elucidation, and bioactivity evaluation of **1**–**8** was reported.

2. Materials and methods

2.1. General experimental procedures

Optical rotations were measured on a JASCO P2000 automatic digital polarimeter. UV spectra were obtained on a JASCO V-650 spectrophotometer, IR spectra were recorded on a Nicolet 5700 spectrometer, and ECD spectra were acquired on a JASCO J-815 spectrometer. NMR experiments were performed on Bruker AV-III 500, VNS-600, and Bruker AV-600 spectrometers in DMSO. HRESIMS data were collected on an Agilent 1100 series LC/MSD ion trap mass spectrometer. Analytical HPLC experiments was carried out on an Agilent 1100 with YMC-Pack ODS-C18 column (150 × 4.6 mm, 5 μm) and YMC-Pack ODS-C8 column (250 × 4.6 mm, 5 μm) at a flow rate of 1 mL/min. MPLC experiments were conducted on a Büchi system consisting of two pumps (C-605), a UV detector (C-635), and an ODS column (60 × 600 mm, 50 μm, 400 g; YMC). Preparative HPLC separations were performed on a Shimadzu LC-6AD instrument with a UV detector (SPD-10A), an ODS-C18 column (250 × 20 mm, 5 μm, YMC). Column chromatography (CC) was performed with Silica gel (200–300 mesh, Qingdao Marine Chemical Inc., Qingdao, China), Chiral AD-H column (4.6 mm × 250 mm, 5 μm, Daicel, Japan) and ODS (50 μm, YMC, Japan). Precoated silica gel GF254 plates were used for TLC, and UV light or spraying with 10% sulfuric acid in EtOH followed by heating is used for spots.

2.2. Plant material

The barks of *Magnolia officinalis* var. *biloba* were collected in Fujian, China, in September 2016. A voucher specimen (ID-S-2898) was identified by D.r Lin Ni from Fujian Agriculture and Forestry University and was deposited at the herbarium of the Institute of Material Medica, Chinese Academy of Medical Sciences and Peking Union Medical College, China.

2.3. Extraction and isolation

The dried barks of *Magnolia officinalis* var. *biloba*. (25 kg) were extracted with 95% ethanol/H_2O (100 L × 2 h × 3). After evaporation of ethanol in vacuo, the aqueous residue was diluted with water and then partitioned with CH_2Cl_2 (30 L × 3). The CH_2Cl_2 extract (1810 g) was subjected to column chromatography on silica gel with PE–Ethyl acetate to afford 4 fractions (Fr. A1–Fr. A4; 10:1, 4:1, 1:1, 1:2). Fraction A1 was suspended with MeOH and then partitioned with Petroleum ether (10 L × 3). The Methanol extraction (500 g) was separated by a silica gel column (200–300 mesh) eluted with PE–Acetone to afford six sub-fractions (Fr. B1–Fr.B6; 40:1, 20:1, 10:1, 7:1, 5:1, 2:1). Combination of sub-fractions B1 and B2 (122 g) was separated by a silica gel column using PE–EtOAc afforded 9 sub-fractions (Fr. C1–Fr. C6; 100:1, 100:3, 100:5, 100:7, 10:1, 10:4, 10:6, 10:8, 1:1). Fraction C4 (21.6 g) was fractionated using a Sephadex LH-20 column with MeOH–CH_2Cl_2 (v/v 1:1) as eluent to give 10 sub-fractions (D1–D10), Fraction D_5 (8.2 g) was purified by the RP-18 column with MeOH–H_2O (78–95%, step gradients) system and obtaining 20 sub-fractions (Fr.E 1-Fr.E20). Fr. E13 purified by preparative HPLC (65% MeCN –H_2O, detected at 210 nm, 8 mL/min) to give **1** (3.2 mg, t_R = 92 min). HPLC separation was taken on the chiral AD-H column with 10% 2-propanol/*n*-hexane yielded (−)-**1** (0.8 mg, t_R = 11.9 min, 1 mL/min) and (+)-**1** (1.1 mg, t_R = 12.9 min, 1 mL/min). Fraction E15 was purified using preparative HPLC (70% MeCN–H_2O, detected at 210 nm, 8 mL/min) to give **2** (5.8 mg, t_R = 46 min). HPLC separation was taken on the chiral AD-H column with 10% 2-propanol/*n*-hexane yielded (−)-**2** (1.8 mg, t_R = 8.7 min, 1 mL/min) and (+)-**2** (2.0 mg, t_R = 10.9 min, 1 mL/min). Fraction E17 was purified by preparative HPLC (detected at 210 nm, 8 mL/min) to give **6** (10.1 mg, t_R = 35 min), **5** (6.4 mg, t_R = 46 min). HPLC separation was taken on the chiral AD-H column with 18% 2-propanol/*n*-hexane yielded (−)-**5** (2.1 mg, t_R = 8.9 min, 1 mL/min) and (+)-**5** (1.8 mg, t_R = 10.5 min, 1 mL/min). Fraction E18 was purified by preparative HPLC (detected at 210 nm, 8 mL/min) to give **3** (5.2 mg, t_R = 35 min), **4** (5.8 mg, t_R = 41 min), **7** (4.7 mg, t_R = 49 min), HPLC separation was taken on the chiral AD-H column with 10% 2-propanol/*n*-hexane yielded (+)-**3** (1.4 mg, t_R = 11.9 min, 1 mL/min) and (−)-**3** (2.0 mg, t_R = 13.4 min, 1 mL/min), HPLC separation was taken on the chiral AD-H column with 15% 2-propanol/*n*-hexane yielded (+)-**4** (1.2 mg, t_R = 11.9 min, 1 mL/min) and (−)-**4** (1.8 mg, t_R = 12.9 min, 1 mL/min). Fraction E20 was purified by preparative HPLC (detected at 210 nm, 8 mL/min) to give **8** (4.7 mg, t_R = 56 min).

2.3.1. Magmenthane A (1)

Colorless oil; (+)-Magmenthane A; [α]20 D + 10.1 (*c* 0.01 MeOH); (−)-Magmenthane A; [α]20 D − 20.0 (*c* 0.05 MeOH); UV (MeOH) λ_{max} (log ε) 294 (0.29) nm; IR (microscope) ν_{max} 3345, 2958, 1668, 1596, 1257, 911, 826,751 cm^{-1}; ^1H NMR and ^{13}C NMR data were showed in Tables 1 and 2, respectively. HRESIMS *m/z* 439.2253 $[M + Na]^+$ (calcd for $C_{28}H_{34}O_3Na$, 439.2244).

2.3.2. Magmenthane B (2)

Colorless oil, (+)-Magmenthane B, [α]20 D + 20.6 (c 0.1 MeOH); (−)-Magmenthane B, [α]20 D − 22.8 (c 0.1 MeOH), UV (MeOH) λ_{max} (log ε) 255 (0.41) nm; IR (microscope) ν_{max} 3348, 2957, 1672, 1260, 913, 821 cm^{-1}; ^1H NMR and ^{13}C NMR data were showed in Tables 1 and 2, respectively. HRESIMS *m/z* 439.2259 $[M + Na]^+$ (calcd for $C_{28}H_{32}O_3Na$, 439.2244).

2.3.3. Magmenthane C (3)

Colorless oil, (+)-Magmenthane C, [α]20 D + 35.6 (c 0.1 MeOH); (−)-Magmenthane C, [α]20 D − 30.1 (c 0.1 MeOH); UV (MeOH) λ_{max} (log ε) 280 (0.10) nm; IR (microscope) ν_{max} 3302, 2961, 1669, 1494, 1048, 915, 823 cm^{-1}; ^1H NMR and ^{13}C NMR data were showed in Tables 1 and 2, respectively. HRESIMS *m/z* 441.2417 $[M + Na]^+$ (calcd for $C_{28}H_{34}O_3Na$, 441.2400).

2.3.4. Magmenthane D (4)

Colorless oil; (+)-Magmenthane D, [α]20 D + 52.4 (c 0.1 MeOH); (−)-Magmenthane D, [α]20 D − 62.3 (c 0.1 MeOH); UV (MeOH) λ_{max}

Table 1
^{1}H NMR spectroscopic data of compounds **1–8.**

Position	**1**[a]	**2**[a]	**3**[a]	**4**[a]	**5**[a]	**6**[a]	**7**[b]	**8**[b]
2	6.91, d (1.2)	6.96, d (2.4)	6.92, brs	7.02, d (2.4)	7.01, d (1.8)	6.97, brs	6.24, d (1.8)	6.26, d (1.8)
5		6.97, d (8.4)	7.06, d (7.2)	7.06, d (7.8)	6.94, d (8.4)	6.96, brs		
6	7.14, d (1.2)	7.05, dd (2.4, 8.4)	7.05, brt, (1.8, 7.2)	7.00, brt (2.4)	6.98, dd (2.4, 8.4)	7.03, brd (6.4)	6.52, d (1.8)	6.51, d (1.8)
7	3.28, brs	3.28, brs	3.28, brd (7.2)	3.28, brs	3.27, brd (6.6)	3.28, brd (7.2)	3.19, brd (6.6)	3.20, brd (6.6)
8	5.90, m	5.87, m	5.90, m	5.90, m	5.90, m	5.91, m	5.86, m	5.93, m
9	5.09, m	5.00, m	5.04, m	5.10, m	5.07, m	5.05, m	4.99, m	5.00, m
10			−OH, 3.92, s			−OH, 4.58		
11	2.77, d (10.8)	4.89, s	4.39, d (4.2)	3.86, brs	3.27	4.16, d (5.4)	4.02, dd	4.09, d (4.2)
				−OH, 4.42	−OH, 4.64		(3.6, 10.8)	
12	2.97, m	3.10, s	5.41, d (4.2)	5.10, d (1.2)	1.35, m	1.61, m	1.77, m	5.49, d (4.2)
	−OH, 4.99				1.62, m	1.65, m	2.11, brd (3.6)	
13	1.90, dd				2.14, m	1.71, m	2.13, brd (3.0)	
	(1.8, 9.6)							
14	5.69, dd	5.13, brs	1.89, m	1.72, m	1.25, m	5.40, d (10.2)	5.56, dd (3.0, 10.2)	1.94, m
	(0.6, 10.4)		1.99, m	1.84, m	1.38, m			2.14, m
15	5.81, dd (2.4, 7.2)	2.32, brs	1.37, m	1.33, m	1.48, m	5.33, d (10.2)	5.52. dd (1.2, 10.2)	1.57, m
		2.33, brs	1.58, m	1.38, m	1.54, m			1.98, m
16	2.17, m	2.09, m	2.09, m	2.05, m	1.51, m	1.47, m	1.53, m	2.08, m
17	0.63, d (7.2)	0.88, d (1.8)	0.86, d (7.2)	0.87, d (6.6)	1.58, s	0.75, 3H, t (7.2)	0.83, d (6.6)	0.89, t (7.2)
18	0.94, d (7.2)	0.87, d (2.4)	0.88, d (7.2)	0.88, d (6.6)	4.56, d (16.8)	0.76, 3H, t (7.2)	0.81, d (7.2)	0.89, t (7.2)
					4.59, d (16.8)			
19	1.25, s	1.25, s	1.03, s	0.89, s	0.89, s	0.99, 3H, s	1.29, s	1.11, s
2′	6.94, d (1.8)	6.89, brs	6.87, d (2.4)	6.90, brs	6.88, brs	6.84, brs	7.10, d (8.4)	7.10, d (8.4)
3′							6.83, d (8.4)	6.82, d (8.4)
4′	−OH, 8.98	−OH, 8.99	−OH, 9.17	−OH, 8.79	−OH, 8.80	−OH, 8.83		
5′	6.76, d (7.8)	6.77, d (8.4)	6.78, d (7.8)	6.77, d (9.0)	6.75, d (7.8)	6.73, d (7.8)	6.83, d (8.4)	6.82, d (8.4)
6′	6.90, dd (1.8, 7.8)	6.91, brt (2.4)	6.91, dd (2.4, 7.8)	6.91, brt (2.4)	6.89, brt (1.8)	6.86, brt (8.4)	7.10, d (8.4)	7.10, d (8.4)
7′	3.22, brd (7.2)	3.22, brd (7.2)	3.23, brd (7.2)	3.23, brd (7.2)	3.22, brd (7.2)	3.19, brd (6.6)	3.32, brd (7.8)	3.32, brs
8′	5.86, m	5.93, m	5.92, m	5.88, m	5.86, m	5.85, m	5.95, m	5.87, m
9′	4.97, m	5.03, m	4.98, m	4.99, m	4.95, m	4.95, m	5.05, m	5.00, m

[a] Recorded at 600 MHz for ^{1}H in DMSO-d_6.
[b] Recorded at 600 MHz for ^{1}H in CD_3OD, δ_H, mult (J in Hz).

(log ε) 291 (0.10) nm; IR (microscope) ν_{max} 3322, 2959, 1671, 1493, 918, 823, 1042 cm^{-1}; ^{1}H NMR and ^{13}C NMR data were showed in Tables 1 and 2, respectively. HRESIMS *m/z* 441.2417 [M + Na]$^{+}$ (calcd for $C_{28}H_{34}O_3Na$, 441.2400).

2.3.5. Magmenthane E (5)

Colorless oil; (+)-Magmenthane E, [α]20 D + 42.2 (c 0.1 MeOH); (−)-Magmenthane E, [α]20 D − 38.8 (c 0.1 MeOH); UV (MeOH) λ_{max} (log ε) 291 (0.30) nm; IR (microscope) ν_{max} 3273, 2962, 1672, 1492, 1269, 914, 821 cm^{-1}; ^{1}H NMR and ^{13}C NMR data were showed in Tables 1 and 2, respectively. HRESIMS *m/z* 441.2385 [M + Na]$^{+}$ (calcd for $C_{28}H_{34}O_3Na$, 441.2400).

2.3.6. Magmenthane F (6)

Colorless oil, (+)-Magmenthane F, [α]20 D + 22.0 (c 0.1 MeOH); UV (MeOH) λ_{max} (log ε) 255 (0.41) nm; IR (microscope) ν_{max} 3374, 2963, 1673, 1495, 1277, 914, 822 cm^{-1}; ^{1}H NMR and ^{13}C NMR data were showed in Tables 1 and 2, respectively. HRESIMS *m/z* 441.2416 [M + Na]$^{+}$ (calcd for $C_{28}H_{34}O_3Na$, 441.2400)

2.3.7. Magmenthane G (7)

Colorless oil; [α]20 D + 44.0 (c 0.1 MeOH); UV (MeOH) λ_{max} (log ε) (0.60), 221 (0.44), 302 (0.13) nm; IR (microscope) ν_{max} 3340, 2969, 1672, 1503, 1218, 917,832 cm^{-1}; ^{1}H NMR and ^{13}C NMR data were showed in Tables 1 and 2, respectively. HRESIMS *m/z* 457.2366 [M + Na]$^{+}$ (calcd for $C_{28}H_{34}O_4Na$, 457.2349).

2.3.8. Magmenthane H (8)

Colorless oil; [α]20 D – 40.1 (c 0.1 MeOH); UV (MeOH) λ_{max} (log ε) 275 (0.09) nm; IR (microscope) ν_{max} 3257, 2964, 1579, 1502, 1218,

Table 2
^{13}C NMR spectroscopic data of compounds **1–8.**

Position	**1**[a]	**2**[a]	**3**[a]	**4**[a]	**5**[a]	**6**[a]	**7**[b]	**8**[b]
1	130.1	131.9	131.5	133.8	133.2	131.3	136.2	136.3
2	129.9	132.4	132.0	131.9	132.0	132.0	111.3	111.6
3	121.0	129.3	128.7	127.8	133.3	129.3	149.7	149.0
4	153.2	154.1	154.1	151.1	151.6	154.1	136.8	137.2
5	130.9	115.1	113.8	123.9	122.2	114.4	151.3	149.0
6	125.8	128.4	128.5	127.8	127.9	128.3	112.1	111.9
7	40.5	39.1	39.1	39.1	39.2	39.2	39.3	39.3
8	138.7	138.4	138.5	138.3	138.3	138.5	137.1	137.1
9	115.8	116.0	115.9	116.1	116.0	115.9	114.6	114.6
10	86.7	58.6	69.4	82.9	81.3	69.0	71.6	84.0
11	54.3	76.4	77.5	71.0	71.2	80.2	85.8	70.1
12	70.9	57.1	116.9	122.1	33.9	25.8	27.3	117.4
13	47.1	141.2	148.1	143.7	37.1	38.0	40.5	147.3
14	128.6	115.7	32.3	24.7	26.2	129.9	129.8	24.5
15	130.3	27.1	25.0	31.3	31.8	133.3	132.5	31.9
16	25.2	34.3	34.3	33.9	150.4	31.5	32.2	34.3
17	16.4	21.6	21.5	21.6	21.2	20.4	19.2	20.1
18	21.1	21.1	21.6	21.6	108.8	20.0	19.4	20.3
19	27.9	19.8	24.8	18.8	22.6	25.3	21.9	23.5
1′	130.7	129.6	130.3	129.7	129.4	129.3	134.1	134.1
2′	131.4	131.9	131.9	132.3	132.3	132.0	129.3	129.3
3′	124.7	125.8	126.5	126.7	126.3	125.7	117.0	116.7
4′	153.6	153.3	152.8	153.0	153.1	153.1	156.0	156.0
5′	116.1	115.9	116.2	116.2	115.9	115.7	117.0	116.7
6′	128.5	128.4	128.5	128.6	128.4	128.3	129.3	129.3
7′	39.1	39.2	39.1	39.3	39.2	39.2	38.9	38.9
8′	138.6	138.6	138.6	138.8	138.7	138.7	137.7	137.7
9′	115.7	115.7	115.7	115.6	115.6	115.6	114.4	114.3

[a] Recorded at 150 MHz for ^{13}C in DMSO-d_6.
[b] Recorded at 150 MHz for ^{13}C in CD_3OD.

917,818 cm^{-1}; ^1H NMR and ^{13}C NMR data were showed in Tables 1 and 2, respectively. HRESIMS *m/z* 457.2359 $[M + Na]^+$ (calcd for $C_{28}H_{34}O_4Na$, 457.2349).

2.4. PTP1B inhibitory assay

Recombinant human GST-PTP1B protein was overexpressed by hGST-PTP1B-BL-21 *E. coli* and purified by GST affinity chromatography. The pNPP reagent was used as the substrate for the measurement of PTP1B activity. Compounds **1–8** (10 μM) and positive control CC06240 (10 μM), along with compounds **5**, **8** and positive control CC06240 (100 μM, 20 μM, 4.0 μM, 0.8 μM, 0.16 μM, 0.032 μM, and 0.006 μM), were pre-incubated with the enzyme at room temperature for 5 min. Assays were performed in a final volume of 100 μL in the active system containing 50 mM HEPES, 5 mM DTT, 150 mM NaCl, 2 mM EDTA, and 2 mM pNPP (pH 7.0), incubated at 30 °C for 10 min, and terminated by addition of 50 μL of 3 M NaOH. Then, absorbance was determined at 405 nm wavelength. The similar system without GST-PTP1B protein was used as blank. Each concentration of the compounds was tested thrice in parallel. IC_{50} values were calculated using Microsoft Excel software. The positive control exhibited an IC_{50} value of 0.77 μM.

2.5. Neuroprotection assay

Human neuroblastoma SK-N-SH cells were cultured in Dulbecco's modified Eagle's medium (DMEM) containing 10% foetal bovine serum, 100 U/mL penicillin, and 100 μg/mL streptomycin. SK-N-SH cells were incubated in 96-well microplates at a density of 1×10^5 cells/mL at 37 °C in a humidified incubator with 5% CO_2/95% O_2. Compounds **1–8** (10 μM), donepezil (20 μM) and tetraethylammonium (TEA, 20 μM) were prepared in dimethyl sulfoxide (DMSO) and diluted with DMEM. For the L-glutamic acid-induced cell neurotoxicity assay, the cells were pre-incubated with compounds **1–8** and positive controls for 2 h, and then 27 mM L-glutamic acid was added to the cells. For the oxygen glucose deprivation (OGD)-induced cell viability assay, the cells were pre-incubated with compounds **1–8** and positive controls for 2 h, respectively. Then, 2.5 mM/L sodium hyposulfite was added to the cells. After 4 h of co-incubation with L-glutamic acid and/or sodium hyposulfite, MTT solution (5 mg/mL) was added for another 4 h at 37 °C; MTT formazan crystals were then solubilized by 150 μL DMSO for 20 min and spectrophotometrically measured at 570 nm. Cell viability was expressed as a percentage of the control group. All data presented in our study were obtained from at least three independent experiments and were expressed as the means ± SEM. Significant differences between groups were compared using the one-way ANOVA procedure followed by an LSD post hoc test using SPSS (version 10.0) software. $P < 0.05$ was considered to be statistically significant.

3. Results and discussion

Magmenthane A (**1**) was obtained as colourless oil. The molecular formula, $C_{28}H_{32}O_3$, was deduced from the (+)-HRESI-MS ions at *m/z* 439.2253 $[M + Na]^+$ (calcd for $C_{28}H_{32}O_3Na$, 439.2244), which indicated 13 degrees of unsaturation. The IR spectrum showed absorptions for hydroxyl (3345 cm^{-1}) and double bond (1668 cm^{-1}) groups. With the help of the ^1H–^1H COSY spectrum of **1** (Fig. 1), the ^1H NMR spectrum showed two groups of aromatic proton signals: an AX spin system [δ_H 6.91 (1H, d, J = 1.2 Hz, H-2) and 7.14 (1H, d, J = 1.2 Hz, H-6)] revealing a 1,3,4,5-tetrasubstituted benzene ring in **1**, and an ABX spin system [δ_H 6.94 (1H, d, J = 1.8 Hz, H-2′), 6.76 (1H, d, J = 7.8 Hz, H-5′), and 6.90 (1H, dd, J = 1.8 Hz, 7.8 Hz, H-6′)] suggesting a 1,3,4-trisubstituted benzene ring in **1**, respectively. Two allyl groups [δ_H 3.28 (H-7), 5.90 (H-8), and 5.09 (H-9), and δ_H 3.22 (H-7′), 5.86 (H-8′), and 4.97 (H-9′)], three methyl groups [δ_H 0.63 (H-17), 0.94 (H-18), and 1.25 (H_3-19)], and two hydroxyl groups [(δ_H 4.99 (OH-11) and 8.98 (OH-4′)] were observed in the ^1H NMR spectrum of **1**. The ^{13}C NMR and HSQC spectra displayed 28 carbon resonances, three methyls, four methylenes (including two olefinic carbons), 13 methines (including four olefinic carbons, five aromatic carbons, and one oxygenated carbon), and eight quaternary carbons (including three oxygenated carbons [δ_C 86.7 (C-10), 153.2 (C-4), and 153.6 (C-4′)]. The ^{13}C NMR spectrum included 12 aromatic carbon signals and two allyl group carbon signals, and the two allyl groups were located at two benzene rings [3] by the carbon-carbon bonds of C-1/C-7 and C-1′/C-7′, according to the HMBC correlations (Fig. 1) from H-7 to C-1, C-2, and from H-7′ to C-1′, C-6′, respectively. The HMBC correlations of OH-4′/C-3′, H-2′/C-3, and H-2/C-3′ supporting the two allylbenzenes were connected through a carbon–carbon bond between C-3 and C-3′. The two hydroxyl groups (δ_H 4.99 and 8.98) were designated at C-12 and C-4′ through the HMBC correlations of OH-12/C-11, C-12, C-13, OH-4′/C-3′, C-4′, and C-5′, respectively. On the basis of the above data, the fragment of 4,5-disubstituted-1,1′-di-

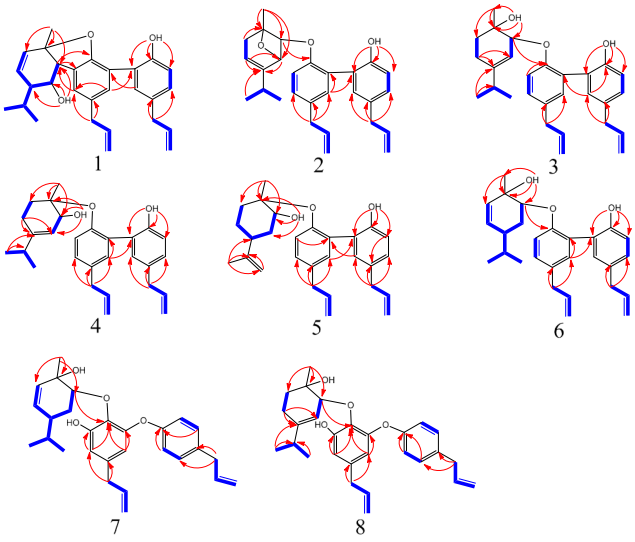

Fig. 1. Key ^1H–^1H COSY (——) and HMBC (⌒) correlations of compounds **1–8**.

allyl-biphenyl-4′-ol was established.

The ^1H–^1H COSY cross peaks of H-11/H-12/H-13/H-14/H-15, H-17/H-16/C-18, and the HMBC correlations from H_3-19 to C-10, C-11, and C-15 gave the structure of a 1-isopropyl-4-methylcyclohexane fragment which was referred to as a *p*-menthane moiety [16]; together with the double bond located at C-14 in molecule **1**, an unsaturated *p*-menthane moiety was confirmed. The key HMBC correlations of H-6/C-11, H-12/C-4 and C-5 revealed C-11 located at C-5. Moreover, a double bond, a 1-isopropyl-4-methylcyclohexane fragment and a 1,1′-diallyl-biphenyl system accounted for 10 degrees of unsaturation; the remaining one degree of unsaturation implies the presence of an additional ring system in **1**, and the HMBC correlation from H-11 to C-4 and the ^{13}C chemical shifts of C-4 (δ_C 153.2) and C-11 (δ_C 70.9) suggested an oxo-bridge between C-4 and C-11. Thus, a ring (C-5–C-4—O—C—10–C-11) was constructed in molecule **1**. The planar structure of compound **1** was elucidated.

The relative configuration of **1** was established by NOESY spectrum (Fig. 2). The NOESY correlations of H_3-19/H-11/H-13 and H-16/H-12 revealed that H-12 and H-16 were on the same side and that OH-12, H-13 and Me-19 were on the opposite side. Optical rotation and no Cotton effect in the electronic circular dichroism (ECD) spectrum of **1** implied that compound **1** was a racemic mixture. Consequently, an AD-H column yielded (+)-**1** and (−)-**1**. The absolute configurations of (+)-**1** and (−)-**1** were determined via comparing the calculated ECD and the experimental ECD of (+)-**1** and (−)-**1**. Moreover, the experimental

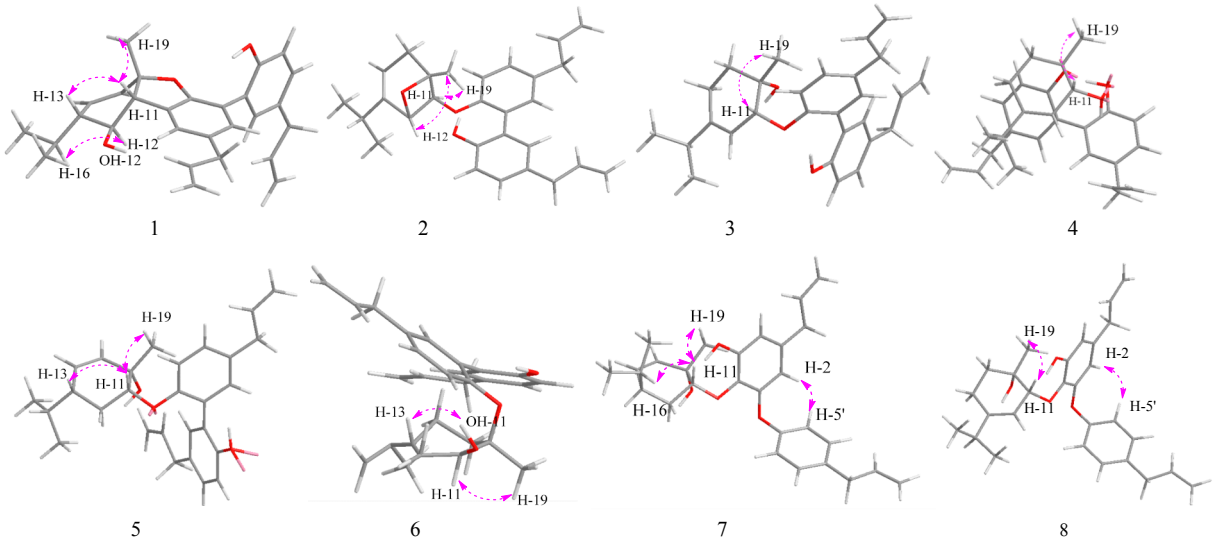

Fig. 2. Key NOESY (↷) correlations of compounds **1–8**.

ECD curves of (+)-**1** and (−)-**1** were in agreement with the calculated ECD [17] curves of 10*S*,11*R*,12*S*,13*R*-**1** and 10*R*,11*S*,12*R*,13*S*-**1**, respectively. Thus, compounds (+)-**1** and (−)-**1** were named as (+)-magmenthane A and (−)-magmenthane A, respectively (see Fig. 3).

The molecular formula of magmenthane B (**2**) was established as $C_{28}H_{32}O_3$ by HRESI-MS ($C_{28}H_{342}O_3Na$, *m/z* 439.2259 $[M + Na]^+$, calcd for $C_{28}H_{32}O_3Na$, 439.2244), which indicated 13 degrees of unsaturation. From analyses of the 1D-NMR and 2D-NMR spectra of **2** (Fig. 1), two 1,3,4-trisubstituted benzene ring systems [δ_H 6.96 (1H, d, J = 2.4 Hz, H-2), 6.97 (1H, d, J = 8.4 Hz, H-5), 7.05 (1H, dd, J = 2.4, 8.4 Hz, H-6) and δ_H 6.89 (1H, brs, H-2′), 6.77 (1H, d, J = 8.4 Hz, H-5′), and 6.91 (1H, brt, J = 2.4 Hz, H-6′)], two allyl groups [δ_H 3.28 (H-7), 5.87 (H-8), and 5.00 (H-9), and δ_H 3.22 (H-7′), 5.93 (H-8′), 5.03 (H-9′)], and three methyls [δ_H 0.87 (H-18), 0.88 (H-17), 1.25 (H-19)] showed in the ^{1}H NMR spectrum. The ^{1}H–^{1}H COSY correlations of H-7/H-8/H-9 and H-7′/H-8′/H-9′, together with the HMBC correlations from H-7 to C-1, C-2, and C-6, from H-7′ to C-1′, C-2′ and C-6′ suggested two allylbenzene fragments [3] in **2**, respectively. In addition, the HMBC correlations between H-5/C-3, H-5′/C-3′, and H-2/C-3 and C-3′ attested to two allylbenzenes were connected by a carbon-carbon bond between C-3 and C-3′. A hydroxyl group (δ_H 8.98, OH-4′) was determined to be located at C-4′ by the HMBC correlations of OH-4′/C-3′, C-4′, and C-5′. The above data established the moiety of 1,1′-diallyl-biphenyl-4′-ol, which was a structural analogue of magnolol [18].

In association with the olefin carbon chemical shifts at δ_C 141.1 (C-13) and δ_C 115.7 (C-14), the HMBC correlations from H-14 to C-10, C-12 and C-13, from H-17 to C-13, from H-19 to C-10, C-11, and C-15, and the ^{1}H–^{1}H COSY correlations of H-14/H-15 and H-17/H-16/H-18 indicated an 1-isopropyl-4-methylcyclohexane moiety in **2**, with the double bond located at C-13 in structure **2**. Likewise, the HMBC cross peak of H-11/C-4 and the characteristic ^{13}C chemical shifts of C-4 at δ_C 154.1 and C-11 at δ_C 76.4 showed the attachment of C-4 to C-11 through an oxygen atom. An unsaturated *p*-menthane moiety and a 1,1′-diallyl-biphenyl-4′-ol moiety in **2** indicated one remaining ring in the structure of **2**. Oxygenated carbons with δ_C 58.4 (C-10) and δ_C 57.1 (C-12) revealed that one oxygen atom connected C-10 and C-12. Thus, the planar structure of **2** was constructed.

The relative stereochemistry of **2** was established through a NOESY spectrum (Fig. 2), which showed correlations of H-11/H_3-19/H-12, indicating that H-11, H-12, and Me-19 were of the *α*-configuration, while H-12 and H-16 were of the *β*-configuration. No Cotton Effect of the ECD of **2** indicated that compound **2** was a racemic mixture. Similarly, HPLC purification in an AD-H column yielded (+)-**2** and (−)-**2**, and the calculated ECD results of 10*R*,11*S*,12*S*-**2** and 10*S*,11*R*,12*R*-**2** matched well with the experimental ECD curves of (+)-**2** and (−)-**2**, which suggested that the absolute structures of (+)-**2** and (−)-**2** were determined as 10*R*,11*S*,12*S*-**2** and 10*S*,11*R*,12*R*-**2**, which were named as (+)-magmenthane B and (−)-magmenthane B, respectively.

For magmenthane C (**3**), the molecular formula of $C_{28}H_{34}O_3$ acquired by HRESI-MS (*m/z* 441.2417, $[M + Na]^+$, calcd for $C_{28}H_{34}O_3Na$, 441.2400) suggested 12 degrees of unsaturation. In combination with the ^{1}H–^{1}H COSY, HSQC and HMBC spectra of **3,** the ^{1}H NMR spectrum showed two sets of 1,3,4-trisubstituted benzene ring proton signals [δ_H 6.92 (1H, brs, H-2), 7.06 (1H, d, J = 7.2 Hz, H-5), and 7.05 (1H, brt, J = 1.8 Hz, 7.2 Hz, H-6) and δ_H 6.87 (1H, d, J = 2.4 Hz, H-2′), 6.78 (1H, d, J = 7.8 Hz, H-5′), and 6.91 (1H, dd, J = 2.4 Hz, 7.8 Hz, H-6′)] and three methyl groups at δ_H 0.86 (3H, d, J = 7.2 Hz, H-17), δ_H 0.88 (3H, d, J = 7.2 Hz, H-18), and δ_H 1.03 (3H, s, H_3-19). One olefin proton signal was observed at δ_H 5.41 (1H, d, J = 4.2 Hz, H-12). The ^{1}H–^{1}H COSY correlations H-7/H-8/H-9, H-7′/H-8′/H-9′ showed two allyl groups in **3**, respectively. The fragment of 1,1′-diallyl-biphenyl-4′-ol was determined through the HMBC correlations from OH-4′ to C-3′, C-4′ and C-5′, from H-2′ to C-3 and C-4′, from H-7 to C-1 and C-2, and from H-7′ to H-1′ and H-2′.

The presence of the 1-isopropyl-4-methylcyclohexane (*p*-menthane) structure was confirmed by the observation of the HMBC correlations (Fig. 2) from H_3-19 to C-10, C-11 and C-15, from OH-10 to C-10, C-11 and C-19, and the ^{1}H–^{1}H COSY correlations of H-11/H-12, H-14/H-15, and H-17/H-16/H-18. The HMBC correlations from OH-10 to C-10, C-12, and C-19 indicated a hydroxyl group located at C-10. The HMBC correlation of H-11/C-4 implies that an oxygen atom linked C-4 and C-11 because of the ^{13}C chemical shifts of C-4 (δ_C 154.1) and C-11 (δ_C 77.5). Therefore, the structure of **3** was established.

The NOESY correlation of H_3-19/H-11 showed that the H-11 and Me-19 were on the same side, while the optical rotation of **3** of zero indicated that **3** was a racemic mixture. Compounds (+)-**3** and (−)-**3** were separated by HPLC via AD-H column, and the calculated ECD curves of 10*R*,11*S*-**3** and 10*S*,11*R*-**3** matched well with the experimental ECD of (+)-**3** and (−)-**3**, respectively. Ultimately, (+)-**3** and (−)-**3** were named as (+)-magmenthane C and (−)-magmenthane C, respectively.

Magmenthane D (**4**) was obtained as colourless oil with the molecular formula $C_{28}H_{34}O_3$, which was established by the HRESI-MS (*m/z* 441.2417 $[M + Na]^+$, calcd for $C_{28}H_{34}O_3Na$, 441.2400). After

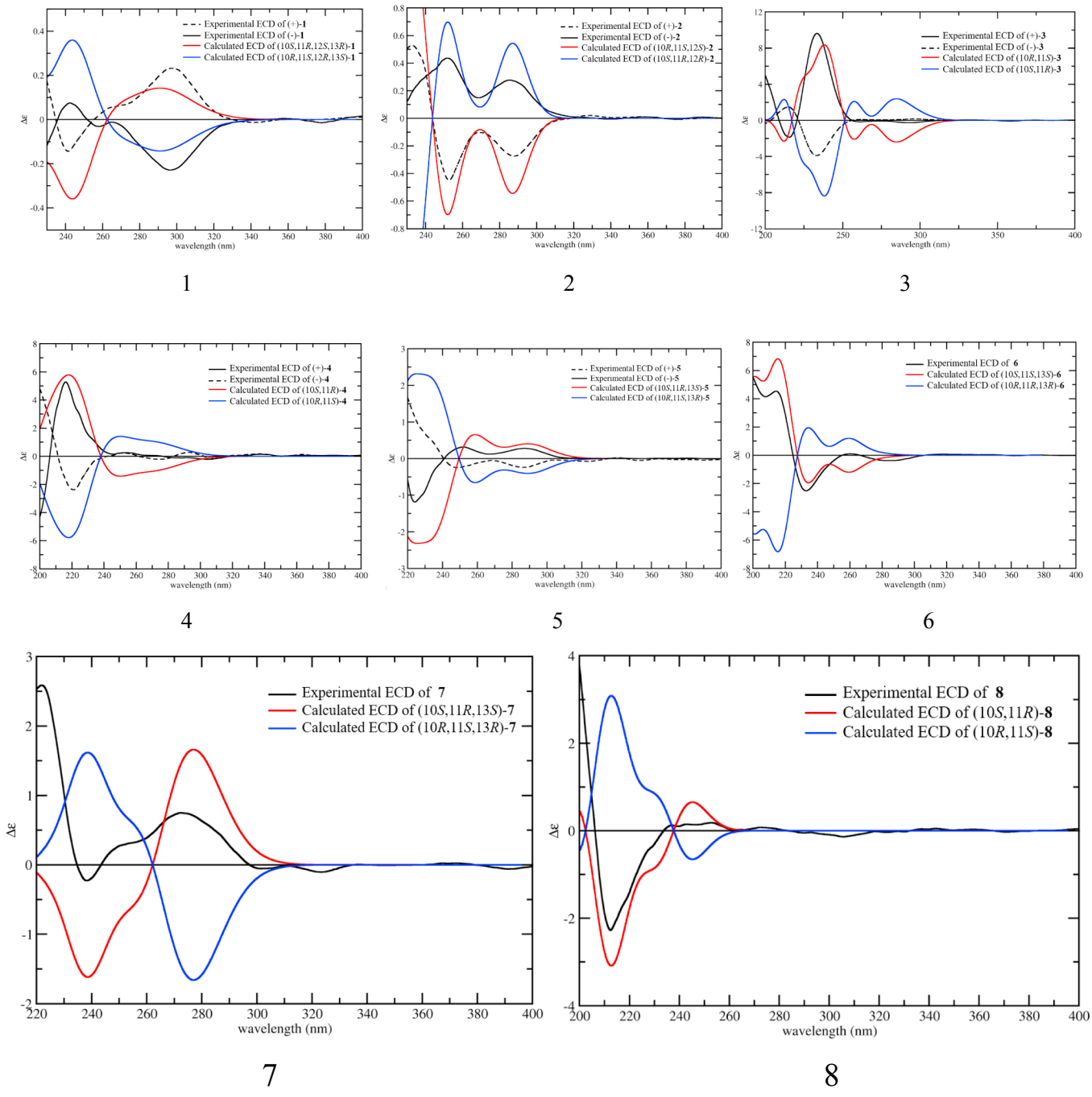

Fig. 3. Comparison of calculated and experimental ECD spectra of compounds **1**–**8**.

analysing the ^{1}H NMR and ^{13}C NMR spectroscopic data (Tables 1 and 2), The 1D-NMR data of **4** closely resembled those of **3**, revealing that they are structurally similar. The key HMBC correlations from H-7 to C-1, C-2 and C-6, from H-7′ to C-1′, C-2′ and C-6′, from OH-4′ to C-3′, C-4′ and C-5′, and from H-2 to C-3′ attested to the structure of 1,1′-diallyl-biphenyl-4′-ol. The HMBC correlations regarding OH-11/C-10, C-11 and C-12 imply that the hydroxyl group was assigned to C-11. In combination with the ^{1}H–^{1}H COSY correlations of H-11/H-12 and H-14/H-15, the key HMBC correlations from H-17 to C-13 and C-16 and from H-19 to C-10, C-11 and C-15 constructed a fragment of unsaturated *p*-menthane, and the oxygenated C-10 (δ_C 82.9) and C-4 (δ_C 151.1) atoms, as well as an additional oxygen atom in **4**, indicated that an oxygen atom connected C-4 and C-10. Hence, the planar structure of **4** was determined.

The NOESY (Fig. 2) correlations of H-11/H_3-19 revealed that the H-11 and C-19 were on the same side. Likewise, chiral HPLC with AD-H column separation produced compounds (+)-**4** and (−)-**4**. The absolute configurations of (+)-magmenthane D and (−)-magmenthane D were determined by comparing the calculated ECD results of 10*S*,11*R*-**4** and 10*R*,11*S*-**4** with the experimental ECD of (+)-**4** and (−)-**4,** respectively.

Magmenthane E (**5**) was obtained as colourless oil with the molecular formula $C_{28}H_{34}O_3$, which was established by HRESI-MS (sodium adduct molecular ion peak at *m/z* 441.2417 $[M + Na]^+$, calcd for $C_{28}H_{34}O_3Na$, 441.2400). Careful analysis of the ^{1}H NMR and ^{13}C NMR spectroscopic data determined that compound **5** contains a fragment of 1,1′-diallyl-biphenyl-4′-ol, which was described previously as compound **3**. The HMBC correlations from H-5/H-2′ to C-3, from H-2′ to C-

Table 3
Neuroprotective effect of compounds **1–8** on glutamic acid induced injury of SK-N-SH cells (10 μM, means ± SD, n = 3, $^{***}p < 0.001$ VS Control).

Group	N value	Mean ± SD	Survival Rate
Control	3	0.793 ± 0.11	–
Model	3	0.374 ± 0.03**	47.2%
Donepezil	3	0.359 ± 0.04	45.3%
TEA	3	0.367 ± 0.03	46.2%
1	3	0.389 ± 0.04	49.1%
2	3	0.348 ± 0.08	43.9%
3	3	0.414 ± 0.04	52.2%
4	3	0.401 ± 0.05	50.6%
5	3	0.431 ± 0.08	54.4%
6	3	0.362 ± 0.01	45.6%
7	3	0.390 ± 0.06	49.2%
8	3	0.342 ± 0.04	43.1%

3, and from OH-4′ to C-3′, C-4′ and C-5′ established the structure of the 4-*O*-1,1′-diallyl-biphenyl-4′-ol fragment.

The ^{1}H–^{1}H COSY correlations of H-11/H-12/H-13/H-14 and key HMBC correlations from H-19 to C-11, C-12 and C-15 and from H-17 to C-13, C-16 and C-18 constructed the fragment of an unsaturated monocyclic monoterpenoid (an unsaturated *p*-menthane moiety), and the oxygenated C-11 (δ_C 71.2) and HMBC correlations from OH-11 to C-10, C-11 and C-12 imply that the hydroxyl group was assigned to C-11. The presence of an additional oxygen atom in the molecule and the chemical shifts of C-4 (δ_C 151.6) and C-11 (δ_C 71.2) prompted postulation of an oxygen atom between C-11 and C-4. Hence, a 1,1′-diallyl-biphenyl-4′-ol fragment and an unsaturated *p*-menthane moiety were connected by an oxygen atom.

The relative configuration of **5** based on its NOESY spectrum (Fig. 2) and the NOESY correlations of H-13/OH-12/H_3-19 revealed that H-13, OH-12, and Me-19 were on the same side. The optical rotation of **5** was determined to be zero, suggesting that compound **5** was a racemic mixture. Chiral HPLC with the AD-H column purified (+)-**5** and (−)-**5**. In addition, the experimental ECD curves of (+)-**5** and (−)-**5** corroborated the calculated ECD curves of 10*S*,11*R*,13*S*-**5** and 10*R*,11*S*,13*R*-**5**, respectively. Therefore, the absolute configurations of (+)-magmenthane E and (−)-magmenthane E were determined.

Magmenthane F (**6**) was obtained as colourless oil. Its molecular formula was established as $C_{28}H_{34}O_3$ by HRESI-MS (ion peak at *m/z* 441.2416 $[M + Na]^+$, calcd for $C_{28}H_{34}O_3Na$, 441.2400). The IR spectrum indicated hydroxyl and double bond absorptions at 3374 and 1673 cm^{-1}, respectively. The ^{1}H NMR and ^{13}C NMR spectroscopic data were similar to those described previously for compound **3**, except that the position of the double bond was at 14, not 12. The ^{13}C NMR spectrum, containing 12 aromatic carbon signals and two allyl group carbon signals, revealed a 4-*O*-1,1′-diallyl-biphenyl-4′-ol moiety which was determined through the HMBC correlations of H-2/C-2 and C-3′ and 4′–OH/C-3′, C-4′, and C-5′. Two allylbenzenes and a double carbon-carbon bond accounted for 11 degrees of unsaturation, while the remaining one degree of unsaturation indicated one ring in **6**.

The ^{1}H–^{1}H COSY correlations between H-11/H-12/H-13/H-14/H-15 and H-17/H-16/H-18, and the HMBC correlations from HO-10 to C-10, C-11, and C-12 and from H_3-19 to C-10, C-11, and C-15 constructed an unsaturated *p*-menthane moiety. The chemical shifts of C-4 at δ_C 154.1 and C-11 at δ_C 80.2 and the HMBC cross peak of H-11/C-4 showed that the C-4 and C-11 were connected by an oxygen atom. Thus, the structure of **6** was constructed. The NOESY correlations of H_3-19/H-11/H-13 indicated that H-11, H-13 and C-19 were on the same side. The absolute configuration of **6** was determined through the comparison of the calculated ECD of 10*S*,11*S*,13*S*-**6** and the experimental ECD of **6**, namely, magmenthane F.

The molecular formula of magmenthane G (**7**) was established as $C_{28}H_{34}O_4$ via HRESI-MS (*m/z* 457.2366 $[M + Na]^+$, calcd for $C_{28}H_{34}O_4Na$, 434.2349), which indicated 12 degrees of unsaturation. With the help of HSQC, the ^{1}H NMR spectrum revealed an AX spin system [δ_H 6.24 (1H, d, J = 1.8 Hz, H-2), 6.52 (1H, d, J = 1.8 Hz, H-6)] and an A_2B_2 spin system [δ_H 7.10 (2H, d, J = 8.4 Hz H-2′, H-6′), 6.83 (2H, d, J = 8.4 Hz, H-3′, H-5′)], along with two allyl groups [δ_H 3.19, 5.86, 4.99 and δ_H 3.32, 5.95, 5.05]. The ^{13}C NMR spectrum, with 12 aromatic carbon signals and two allyl group carbon signals, revealed two allylbenzene fragments, and the HMBC correlations from H-2 to C-1, C-3, C-4, and C-7, from H-6 to C-2, C-4, and C-5, and the ^{1}H–^{1}H COSY correlations between H-7/H-8/H-9 indicated a 3,4,5-trisubstituted-1-allyl-benzene fragment. The HMBC correlations from H-2′ to C-4 and C-7, from H-3′ to C-4 and C-1, and the ^{1}H–^{1}H COSY correlations of H-2′/H-3′, H-5′/H-6′, and H-7′/H-8′/H-9′ revealed the 4′-*O*-1′-allyl-benzene fragment in **7**. The NOESY spectrum correlations (Fig. 2) between H-2 and H-5′ indicated that oxygenated C-3 and C-4′ were connected by an oxygen atom, which connected the fragments of 3,4,5-trisubstituted-1-allyl-benzene and 4′-*O*-1′-allyl-benzene. The ^{1}H–^{1}H COSY correlations of H-11/H-12/H-13/H-14/H-15, H-17/H-16/H-18 and the HMBC correlations from H-19 to C-10, C-11, and C-15 showed the presence of an unsaturated *p*-menthane moiety. The HMBC correlation of H-11/C-4 implies that an oxygen atom connected the C-4 and C-11 because of the chemical shifts of C-4 (δ_C 136.8) and C-11 (δ_C 85.8).

Moreover, the NOESY (Fig. 2) correlations of H_3-19/H-11/H-16 revealed Me-19, H-11, and C-16 on the same side, and the absolute configuration of **7** was determined by comparing the spectrum of the calculated ECD of 10*S*,11*R*,13*S*-**7** and the experimental ECD of **7**. The structure of **7** was determined as 10*S*,11*R*,13*S*-**7** and named magmenthane G.

The molecular formula of magmenthane H (**8**) was established as $C_{28}H_{34}O_4$ via HRESI-MS (*m/z* 457.2359 $[M + Na]^+$, calcd for $C_{28}H_{34}O_4Na$, 457.2349). Fully analysing the 1D and 2D NMR data of **8** revealed that compound **8** was similar to **7**, except that the position of the double carbon–carbon bond was 12, not 14. The ^{1}H NMR spectrum revealed two sets of aromatic proton systems [δ_H 6.26 (1H, d, J = 1.8 Hz, H-2), 6.51 (1H, d, J = 1.8 Hz, H-6) and δ_H 7.10 (2H, d, J = 8.4 Hz, H-2′, H-6′), 6.82 (2H, d, J = 8.4 Hz, H-3′, H-5′)] and two allyl groups [δ_H 3.20, 5.93, 5.00 and δ_H 3.32, 5.87, 5.00]. The NOESY spectrum (Fig. 2) showed the correlations between H-2 and H-5′, attesting that the oxygenated C-3 and C-4′ were connected by an oxygen atom. The ^{1}H–^{1}H COSY correlations between H-11/H-12/H-13/H-14/H-15, and the HMBC correlations from H-19 to C-10, C-11, and C-15 and from H-17/H-18 to C-16, showed the presence of an unsaturated *p*-menthane moiety. The HMBC correlation of H-11/C-4 implies an oxygen atom between C-4 and C-11 because of the chemical shifts of C-4 (δ_C 137.2) and C-11 (δ_C 70.1). The NOESY correlation of H-11/H_3-19 implies that the H-11 and Me-19 are on the same side. The absolute configuration of **8** was determined by comparing the curve of the calculated ECD of 10*S*,11*R*-8 and the curve of the experimental ECD of **8**, named as magmenthane H.

Compounds **1–8** were evaluated for their inhibitory effects against PTP1B, and compounds **5** and **8** (at seven concentration gradients) exhibited significant PTP1B inhibitory activities, with IC_{50} values of 4.38 and 3.80 μM, respectively. At a concentration of 10 μM, compounds **1–8** showed 28.6%, 64.1%, 40.5%, 11.7%, 90.9%, 26.4%, 22.4%, and 87.3% PTP1B inhibitory activities, respectively. Moreover, compounds **1–8** were assessed with respect to neuroprotective effects [19] against glutamic acid- and oxygen glucose deprivation (OGD)-induced SK-N-SH cell injury. At a concentration of 10 μM, compounds **1**, **3–5,** and **7** showed more neuroprotective activities than the positive control drugs donepezil and TEA (45.3% and 46.2%) against glutamic acid-induced SK-N-SH cell injury (Table 3). Compounds **4, 5,** and **7** showed greater efficacy than the positive control drugs donepezil and TEA (62.8% and 60.8%) against OGD-induced SK-N-SH cell injury (Table 4).

Table 4
Neuroprotective effect of compounds 1–8 on ODG-induced injury of SK-N-SH cells (10 μM, means ± SD, n = 3, $^{***}p < 0.001$ VS Control).

Group	N value	Mean ± SD	Survival Rate
Control	3	1.775 ± 0.24	–
Model	3	1.109 ± 0.08*	62.5%
Donepezil	3	1.100 ± 0.12	62.0%
TEA	3	1.080 ± 0.10	60.8%
1	3	1.098 ± 0.07	61.9%
2	3	1.065 ± 0.09	60.0%
3	3	1.031 ± 0.01	58.1%
4	3	1.230 ± 0.06	69.3%
5	3	1.146 ± 0.12	64.6%
6	3	1.064 ± 0.09	59.9%
7	3	1.244 ± 0.03	70.1%
8	3	1.021 ± 0.14	57.5%

Notes

The authors declare no competing financial interests.

Acknowledgments

This work was supported by the National Natural Science Foundation of China (No. 81730093), the CAMS Innovation Fund for Medical Sciences (No. 2016-I2M-2-003), and the CAMS Initiative for Innovative Medicine Project (CAMS-I2M-1-010), In dependent project of State Key Laboratory of Bioactive Substance and Function of Natural Medicines (GTZA201803).

Appendix A. Supplementary material

This material (1D and 2D NMR, UV, IR, and HRESIMS spectra of compounds **1–8**) is provided in the Supporting Information. Supplementary data to this article can be found online at https://doi.org/10.1016/j.bioorg.2019.102948.

References

[1] National Pharmacopoeia Committee, Pharmacopoeia of Peoples Republic of China. Part 1, Chemical Industry Press, Beijing,, 2015, pp. 251–252.
[2] W.L. Kuo, C.Y. Chung, T.L. Hwang, J.J. Che, Phytochemistry 85 (2013) 153–160.
[3] H.C. Shih, P.C. Kuo, S.J. Wu, T.L. Hwang, H.Y. Hung, D.Y. Shen, P.C. Shieh, Y.R. Liao, E.J. Lee, Q. Gu, K.H. Lee, T.S. Wu, Bioorg. Med. Chem. 24 (2016) 1439–1445.
[4] U.J. Youn, Q.C. Chen, W.Y. Jin, I.S. Lee, H.J. Kim, J.P. Lee, M.J. Chang, B.S. Min, K.H. Bae, J. Nat. Prod. 70 (2007) 1687–1689.
[5] Z.Z. Xue, R.Y. Yan, B. Yang, Phytochemistry 127 (2016) 50–62.
[6] R.Y. Yan, W.H. Wang, J. Guo, H.L. Liu, J.Y. Zhang, B. Molecules 18 (2013) 7739–7750.
[7] Z.F. Guo, X.B. Wang, J.G. Luo, J. Luo, J.S. Wang, L.Y. Kong, Fitoterapia 82 (2011) 637–641.
[8] S.X. Yu, R.Y. Yan, R.X. Liang, W. Wang, B. Yang, Fitoterapia 83 (2012) 356–361.
[9] C. Li, C.J. Li, J. Ma, F.Y. Chen, L. L, X.L. Wang, F. Ye, D.M. Zhang, Org. Lett. 20 (2018) 3682–3686.
[10] L.K. Chao, P.C. Liao, C.L. Ho, E.I. Wang, C.C. Chuang, H.W. Chiu, L.B. Hung, K.F. Hua, J. Agric. Food Chem. 58 (2010) 3472–3478.
[11] T. Nakazawa, T. Yasuda, K. Ohsawa, J. Pharm. Pharmacol. 55 (2003) 1583–1591.
[12] Y.M. Wang, L.D. Kong, Y.M. Chen, Phytother. Res. 19 (2005) 526–529.
[13] L.L. Ge, L. Chen, Q.G. Mo, G. Zhou, X.S. Meng, Y.W. Wang, RSC Adv. 8 (2018) 4362.
[14] M.R. Agharahimi, N.A. LeBel, J. Org. Chem. 60 (1995) 1856–1863.
[15] A. Ikoma, N. Ogawa, D. Kondo, H. Kawada, Y. Kobayashi, Org. Lett. 18 (2016) 2074–2077.
[16] M. Miyazawa, Y. Okuno, S. Nakamura, H. Kosaka, J. Agric. Food Chem. 48 (2000) 5440–5443.
[17] A. Mándi, I.W. Mudianta, T. Kurtán, M.J. Garson, J. Nat. Prod. 78 (2015) 2051–2056.
[18] W. Schuehly, W. Voith, H. Teppner, O. Kunert, J. Nat. Prod. 73 (2010) 1381–1384.
[19] Y.T. Zhang, F.M. Li, Y.Z. Guo, L.R. Jiang, J. Ma, Y. Ke, Z.M. Qian, Eur. J. Pharmacol. 792 (2016) 48–53.